Scaling phenomena in a unitary model of directed propagating waves with applications to one-dimensional electrons in a time-varying potential

Dinko Cule and Yonathan Shapir
Department of Physics and Astronomy, University of Rochester, Rochester, New York 14627
(Received 7 September 1993; revised manuscript received 20 April 1994)

We study a two-dimensional (2D) lattice model of forward-directed waves in which the integrated intensity for classical waves (or probability for quantum mechanical particles) is conserved. The model describes the time evolution of a 1D quantum particle in a time-varying potential and also applies to propagation of electromagnetic waves in two dimensions within the parabolic approximation. We present a closed-form solution for propagation in a uniform system. Motivated by recent studies of nonunitary directed models for localized 2D electrons tunneling in a magnetic field, we then address related theoretical questions of how the interference pattern between constrained forward paths in this unitary model is affected by the addition of phases corresponding to such a magnetic field. The behavior is found to depend sensitively on the value of Φ/Φ_0, where Φ is flux per plaquette and Φ_0 is the unit of flux quantum. For $\Phi/\Phi_0 = p/q$ we find the amplitude to be more collimated the larger the value of q is. We next consider propagation in random forward-scattering media. In particular, the scaling properties associated with the transverse width x of the wave, as a function of its distance t from the point source, are addressed. We find the moments of x to scale with t in a very different way from what is known for either off-lattice unitary or on-lattice nonunitary systems. The scaling of the moments of the probability $[P^n(x,t)]$ (or intensity) at a point $(x = 0, t)$ is found to be consistent with a simple behavior $[P^n(0,t)] \sim t^{-n/2}$. Implications for the behavior of one-dimensional lattice quantum particles in a dynamically fluctuating random potential are discussed.

I. INTRODUCTION

Directed propagation of waves in uniform and nonhomogeneous media has many applications in different branches of physics. Classically they arise in the context of electromagnetic wave propagation (e.g., light propagation in the atmosphere). Quantum mechanically they arise in investigations of hopping transport in insulators. If the preferred direction is identified as time, it also describes the motion of a quantum particle that obeys the time-dependent Schrödinger equation.

In the classical-waves context, directed propagation is obtained within the so-called "parabolic approximation" which is applied in circumstances at which most of the scattering is in the forward direction.[1–5] The equation is parabolic because the second derivative in the direction of propagation (say z) is replaced by a first derivative, and the Maxwell equation for a field $E(x,y,z,t) = \mathrm{Re}[\mathcal{E}(x,y,z,t)e^{i(kz-\omega t)}]$ is replaced by

$$\left(i\frac{\partial}{\partial z} + \frac{1}{2k}\nabla^2 - k\,\mu(x,y,z,t)\right)\mathcal{E}(x,y,z,t) = 0, \quad (1.1)$$

where $\mu(x,y,z,t)$ is a nonuniform index of refraction and $\nabla^2 = \frac{\partial^2}{\partial x^2} + \frac{\partial^2}{\partial y^2}$.

In the applications for classical waves, however, in many instances the absorption of the medium in which the "directed propagation" takes place is negligible. Therefore, the total integrated energy at every latitude z is constant as energy is conserved during the propagation. We denote by unitarity (for obvious reasons) the models in which $|E|^2$ (or $|\Psi|^2$ where Ψ is the wave function of a quantum particle) are conserved. One of the most important issues we address in this work is the drastic difference in the properties of directed propagation between unitary and nonunitary models.[5–7]

To approach systematically the problems associated with directed waves in ordered and random media it was found very beneficial to study lattice models. They are often simpler and more amenable to analytic and numeric calculations than their continuum counterparts. But for these studies to universally apply to systems without an underlying lattice structure as well, the question of whether the continuum behavior is recovered from the lattice on length scales much longer than the lattice spacing should be carefully explored.[7]

In this paper, we introduce a two-dimensional (2D) lattice model for unitary directed propagation and investigate its behavior in uniform, nonhomogeneous and random media. Important differences between the lattice and the continuum description will be emphasized. Despite these differences, the study of lattice models helps in the basic understanding of directed propagation in various environments. Moreover, it provides a rich collection of phenomena with potential applications in lattice systems.

Quantum mechanically the model we study is describing the real time evolution of a one-dimensional quantum particle (we shall use electron to denote all of them) in a time-dependent potential $V(x,t)$

$$\imath\hbar\frac{\partial\psi}{\partial t} = -\frac{\hbar^2}{2m}\frac{\partial^2\psi}{\partial x^2} + V(x,t)\,\psi. \tag{1.2}$$

We shall study here the case of a random potential $V(x,t)$. While early studies concentrated on the continuum version,[8,9] a lattice model was recently extensively investigated by Bouchaud *et al.*[10] To conserve probability on a lattice they employed a different method than ours. From their numerical investigation they reached the conclusion that the wave function has multifractal properties. The difference between the discretization methods and the possibility that they may lead to a different behavior will be discussed in the last section.

Another interesting extension we study here is the discrete equation

$$\psi(x,t+1) = e^{\imath\frac{\alpha t}{2}}\,\psi(x-1,t) + e^{-\imath\frac{\alpha t}{2}}\,\psi(x+1,t). \tag{1.3}$$

The main motivation to study this equation is its close formal connection to another interesting system: that of a tunneling electron on a lattice in the presence of a magnetic field. The directed path approximation is invoked for this case of strongly localized electrons precisely because the wave function decays exponentially. Therefore, the "directed paths" approximation cannot be applied in the unitary case to study the spatial behavior of the wave function $\psi(x,y)$ in 2D. However, because of the interesting behavior[11,12] found in the nonunitary case with a magnetic field, there is a strong motivation to widen our theoretical understanding and to investigate what would be the effect of a "magnetic field" on the unitary model with constrained forward paths. The magnetic field is added to the model by adding the "time-dependent" phases [as described in Eq. (1.3)] as for the tunneling electrons in the nonunitary model (in which t denotes the direction of propagation). It should be emphasized again that the behavior found does not describe the behavior of nonlocalized electrons in a real magnetic field.

The organization of this paper is as follows. In Sec. II the model is introduced and its behavior on a pure (uniform) lattice is explored in Sec. III. Next, we address the question of what will happen to the interference in our model if phases, as if induced by a magnetic field, are added to the bonds. That will be discussed in Sec. IV. Section V is devoted to the effects of disorder on the propagation of directed waves. The last section (VI) is devoted to concluding remarks.

After this project was in progress we learned that the same model has been studied independently by Saul *et. al.* in Ref. 7. To some extent our study overlaps with theirs. In these cases our results also agree with theirs and we therefore limit their discussions to the necessary minimum in order to make our paper self-contained. We mostly expand on new directions and extensions beyond their study.

II. THE MODEL

We shall study the propagation of directed waves on a two-dimensional lattice where the direction of propagation is identified as the "time" axis. Such a lattice is illustrated in Fig. 1. An incoming wave may propagate only along lattice bonds. Each site represents a scatterer described by some scattering S matrix. All scattering matrices are elements of the $U(2)$ group (there are two scattering channels). The wave function $\Psi(t)$ of a propagating wave is defined by a set of $2N$ amplitudes $\psi_n(t)$, $(n = 1,2,\ldots,2N;\ N \geq t)$ taking values on the lattice links. Time t corresponds to the number of steps in the t direction.

At each site the S matrix transforms two incoming amplitudes into two outgoing amplitudes. For example, amplitudes $\psi_n(t+1)$ and $\psi_{n+1}(t+1)$, (see Fig. 1), are related to $\psi_n(t)$ and $\psi_{n+1}(t)$ by a matrix multiplication

$$\begin{pmatrix} \psi_{n+1}(t+1) \\ \psi_n(t+1) \end{pmatrix} = \begin{pmatrix} S_{11}(x,t) & S_{12}(x,t) \\ S_{21}(x,t) & S_{22}(x,t) \end{pmatrix} \begin{pmatrix} \psi_{n+1}(t) \\ \psi_n(t) \end{pmatrix}, \tag{2.1}$$

where x is the transversal position of a scatterer, between the nth and the $(n+1)$th row.

The S-matrix elements are closely related to the potential $V(x,t)$ in Eq. (1.2). One way to discretize Eq. (1.2) is to formulate the problem in terms of scattering matrices assigned only to the discrete set of space-time coordinates. The main advantage of this discretization procedure is that unitarity is manifestly preserved which implies that the norm of the wave function is also preserved (there is no dissipation). A shortcoming of the discretization is the existence of a "light cone" which precludes any spread faster than $\langle x^2\rangle \sim t^2$. For example, $\langle x^2\rangle \sim t^3$ found in the continuum,[8,9] cannot be achieved in this model unless it is generalized to allow "long range" scatterings (not restricted to nearest neighbors).

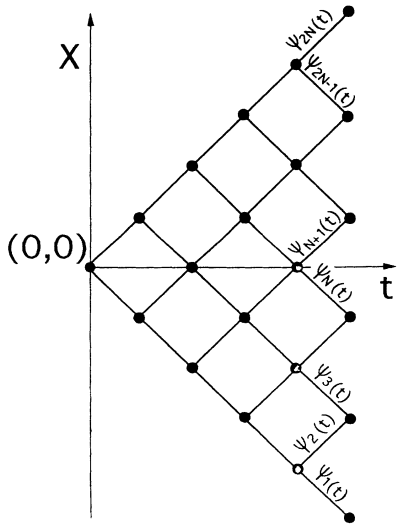

FIG. 1. The lattice description used throughout this work.

III. DIRECTED WAVES ON A PURE LATTICE

In this section, we briefly discuss the wave propagation in the absence of both disorder and an external field. The main goal of this study is to describe analytical methods that will be used in the subsequent sections.

All sites on the lattice will have the same S matrix. As mentioned earlier, it must be a unitary matrix which we choose to have all real elements

$$S = \frac{1}{\sqrt{2}} \begin{pmatrix} 1 & 1 \\ -1 & 1 \end{pmatrix}. \tag{3.1}$$

The transfer matrix T relates wave functions at t and $t-1$

$$\Psi(t) = T\,\Psi(t-1)\,, \tag{3.2}$$

where T is $2N \times 2N$ matrix given by

$$T = \frac{1}{2} \begin{pmatrix} \ddots & & & & & & & \\ & -1 & -1 & -1 & 1 & & & \\ & 1 & 1 & -1 & 1 & & & \\ & & & -1 & -1 & -1 & 1 & \\ & & & 1 & 1 & -1 & 1 & \\ & & & & & & & \ddots \end{pmatrix}. \tag{3.3}$$

The T matrix in Eq. (3.3) takes into account scatterings on two consecutive columns of sites (see Fig. 1). Transfer matrices for each individual column are actually different. Combining them gives the matrix (3.3) which then describes the transfer over two columns. Diagonalizing T by a unitary transformation $T = U^{-1} D\, U$, we have

$$\Psi(t) = U\, D^t\, U^{-1}\, \Psi(t=0). \tag{3.4}$$

Once the wave function $\Psi(t=0)$ at $t=0$ is known one can obtain the wave function at arbitrary t from Eq. (3.4). For example, one can choose as an initial condition a wave function whose components on the first links following the origin have values $1/\sqrt{2}$. This corresponds to an incident wave which at $t=0$ comes to the scatterer at position $x=0$ from below (see Fig. 1) and scatters into an upper or lower link with equal probability $1/2$, see (3.1). Therefore, we have

$$\psi_n(t=0) = \delta_{n,N}\,, \tag{3.5}$$

where $\psi_n(t=0)$ is the nth component of $\Psi(t=0)$, as is shown in Fig. 1.

Note that the scattering matrix given by Eq. (3.1) is not symmetric. This asymmetry of S will produce the asymmetry among the components of the wave function at some later t. One could obtain a symmetric expression for the wave function by an appropriate superposition of another possible initial condition, i.e., the incident wave comes to the first scatterer from above. In the presence of disorder the symmetry will be restored. We also checked numerically that the choice of the initial condition does not have any effect on the scaling exponents.

In order to diagonalize T we impose periodic boundary conditions and choose for definiteness N to be even. The eigenvalues of T are

$$\lambda_\pm = -2\sin^2\frac{k}{2} \pm i2\sqrt{1-\sin^4\frac{k}{2}}\,, \tag{3.6}$$

and components of the eigenvectors E are given by

$$\begin{aligned} E_{2n-1} &= v(k)\, e^{ikn}, \\ E_{2n} &= u(k)\, e^{ikn}, \\ E_{2n+1} &= v(k)\, e^{ik(n+1)}, \\ E_{2n+2} &= u(k)\, e^{ik(n+1)}\,. \end{aligned} \tag{3.7}$$

Here $n = 1,3,\ldots,N-1$; $k = \frac{2\pi}{N}m$, $m = -(\frac{N}{2}-1),\ldots,-1,0,1,\ldots,\frac{N}{2}$, and amplitudes $u(k)$ and $v(k)$ are related by

$$u_\pm = i\,e^{i\frac{k}{2}} \left(-\sin\frac{k}{2} \pm \sqrt{1+\sin^2\frac{k}{2}} \right) v_\pm(k)\,. \tag{3.8}$$

The normalization condition gives

$$|\,u_\pm\,| = \frac{1}{\sqrt{2N}} \left(1+\sin^2\frac{k}{2} \pm \sin\frac{k}{2}\sqrt{1+\sin^2\frac{k}{2}} \right)^{-\frac{1}{2}} \tag{3.9}$$

and

$$|\,v_\pm\,| = \frac{1}{\sqrt{2N}} \left(1+\sin^2\frac{k}{2} \mp \sin\frac{k}{2}\sqrt{1+\sin^2\frac{k}{2}} \right)^{-\frac{1}{2}}. \tag{3.10}$$

Using Eqs. (3.6)–(3.10) it is possible to find the wave function for any t. After a lengthy but straightforward calculation, the even n components are found to be

$$\begin{aligned} \psi_n(t) &= \frac{1}{2^t} \sum_{m=-(\frac{N}{2}-1)}^{\frac{N}{2}} [\lambda_+^t(k_m)\,|\,u_+(k_m)\,|^2 \\ &\quad + \lambda_-^{*t}(k_m)\,|\,u_-(k_m)\,|^2]\, e^{ik_m\frac{n-N}{2}} \\ &= \frac{1}{N} \sum_{m=-(\frac{N}{2}-1)}^{\frac{N}{2}} \left[\cos(\varphi t)\cos\left(k_m\frac{n-N}{2}\right) \right. \\ &\quad \left. + \sin(\varphi t)\frac{\sin k_m}{\sqrt{1+\sin^2\frac{k_m}{2}}} \sin\left(k_m\frac{n-N}{2}\right) \right], \end{aligned} \tag{3.11}$$

while the odd n components are given by

$$\psi_n(t) = -\frac{i}{2^t} \sum_{m=-(\frac{N}{2}-1)}^{\frac{N}{2}} \left[\lambda_+^t(k_m) \left(\sin\frac{k_m}{2} + \sqrt{1+\sin^2\frac{k_m}{2}} \right) \mid u_+(k_m) \mid^2 \right.$$
$$\left. + \lambda_-^{*\,t}(k_m) \left(\sin\frac{k_m}{2} - \sqrt{1+\sin^2\frac{k_m}{2}} \right) \mid u_-(k_m) \mid^2 \right] e^{ik_m(n-N)/2}$$
$$= \frac{1}{N} \sum_{m=-(\frac{N}{2}-1)}^{\frac{N}{2}} \frac{\sin(\varphi t)}{\sqrt{1+\sin^2\frac{k_m}{2}}} \cos\left(k_m \frac{n-N}{2}\right) . \tag{3.12}$$

In the above expressions $\varphi = \arg(\lambda_+)$.

Knowing the closed form for $\Psi(t)$ we can now analytically calculate moments $\langle x \rangle$ and $\langle x^2 \rangle$ as function of t. We have found that for large t

$$\langle x^n \rangle = (1 - \frac{1}{\sqrt{2}})\, t^n , \qquad n = 1, 2 . \tag{3.13}$$

Therefore, we have explicitly reproduced the well known result that in the absence of disorder the wave packet spreads in time in a ballistic way (quantum diffusion), i.e., $\sqrt{\langle x^2 \rangle} \sim t$. In the next section we shall use the same method to study the propagation in an external magnetic field.

IV. INTERFERENCE EFFECTS DUE TO PHASES INDUCED BY A MAGNETIC FIELD

Previous studies[11–15] have addressed the tunneling of strongly localized electrons for which the "directed paths" are justified as an approximation. In these studies a very intriguing behavior was found due to the combined effects of the lattice and the magnetic field on the interfering paths. Therefore, we were compelled to investigate how these combined effects will change in a unitary model, although no direct relation to a realistic system exists for this model. We believe that this study will add to the general understanding of the behavior of lattice electrons in a magnetic field.

The magnetic field adds a phase to the bonds. The phase φ is determined by the applied magnetic field and it is given by the discretized curvilinear integral of the vector potential along the bond between the two sites. There are many possible choices for this phase which yield the same magnetic field and which differ by a gauge transformation. Any gauge such that the sum of all phases around a plaquette gives the correct flux through the plaquette (in units of the flux quantum $\Phi_0 = \frac{\hbar}{e}$) can be used. Here we use the so-called diagonal staggered gauge used in Refs. 11 and 15, $\varphi(t) = \pm\alpha\frac{t}{2}$ with $\alpha = 2\pi\Phi/\Phi_0$ and Φ is the flux per elementary plaquette. The main characteristic of this gauge is that the phase depends linearly on the t coordinate but there is no dependence on the transverse coordinate.

Now we shortly describe the transfer matrix calculations in the presence of a magnetic field. Each step of propagation, say from a site at t to a site at $t+1$ in our notation, includes two bonds, and, therefore, two phases. Let us call them $\varphi_1(t)$ and $\varphi_2(t)$, and denote their combinations by $\varphi_\pm(t) = \varphi_1(t) \pm \varphi_2(t)$. We follow the procedure described in the previous section. In the presence of a magnetic field the basic motif of transfer matrix (3.3) depends on t and it is given by

$$\begin{matrix} -e^{-i\varphi_-} & -e^{i\varphi_-} & -e^{i\varphi_+} & e^{i\varphi_+} \\ e^{-i\varphi_+} & e^{-i\varphi_+} & -e^{i\varphi_-} & e^{i\varphi_-} . \end{matrix} \tag{4.1}$$

In order to diagonalize $T(t)$, we again impose periodic boundary conditions and use the same eigenvectors as before. Simple calculation gives corresponding eigenvalues

$$\lambda_\pm(k,t) = -2\sin\left(\frac{k}{2} - \varphi_1(t)\right) \sin\left(\frac{k}{2} - \varphi_2(t)\right) \pm i\,2\sqrt{1 - \sin^2\left(\frac{k}{2} - \varphi_1(t)\right) \sin^2\left(\frac{k}{2} - \varphi_2(t)\right)} . \tag{4.2}$$

The presence of a magnetic field clearly breaks the standard procedure for transfer matrix calculation. Namely, transfer matrices at different t do not commute and, therefore, cannot be diagonalized simultaneously. However, the product of T matrices which has to be diagonalized can be written in a block-diagonal form with 2×2 matrices on diagonal. Each 2×2 matrix depends on a specific value of transverse momentum vector $k_m = \frac{2\pi}{N} m$. It is defined by a product of 2×2 matrices at different t but with the same value of k. Of course, in the absence of magnetic field, the off-diagonal elements vanish and the diagonal elements are simply $\lambda_+^t(k)$ and $\lambda_-^t(k)$. This suggests the possibility of using the straightforward transfer matrix procedure together with a perturbative treatment for small magnetic field. Perturbative results obtained in this way are too long to be presented here. In the next subsection we will approach the same problem in a different way.

A. Mapping to the Ising model

We now discuss a different approach to the system in the presence of a magnetic field. The basic idea is to map

our model to a one-dimensional Ising model and then to use the transfer matrix techniques to find the partition function which is related to the components of the wave function.

For future use it is now more convenient to consider the transfer over each column of scatterers separately. Thus, we assign a single unitary matrix modified by the effect of a magnetic field to all sites with the same t (the sites along the same column)

$$S = \begin{pmatrix} \alpha_n e^{i\varphi_{n+1}} & \beta_n e^{i\varphi_{n+1}} \\ -\beta_n^* e^{-i\varphi_{n+1}} & \alpha_n^* e^{-i\varphi_{n+1}} \end{pmatrix} . \tag{4.3}$$

α and β are any complex numbers and index $n = 1, 2, \ldots, t$ denotes the position of the scatterer along the t axis. φ_{n+1} is the change of phase of the wave function during the time interval from n to $n+1$. It is positive (negative) for the wave propagating in the up (down) direction, and for our gauge choice it is a linear function of index n.

Again, the probability of reaching point (x,t) is obtained by summing the individual amplitudes of all directed paths starting at the origin and ending at (x,t). To count all different paths we introduce a set of numbers σ_n such that $\sigma_{n+1} = +1$ if the wave scattered at site n goes through the upper bond and $\sigma_{n+1} = -1$ if it goes through the lower bond.[17] The sequence $\sigma_1, \sigma_2, \ldots, \sigma_t$ uniquely specifies a path from the origin to some site at distance t. The final transversal position of a path is given by

$$x = \sum_{n=1}^{t} \sigma_n . \tag{4.4}$$

The value of σ_0 is fixed by the initial condition: $\sigma_0 = +1(-1)$ for the incident wave coming through the lower (upper) bond. Physically, σ_n and x can be identified with spins and the magnetization of the system, respectively. The size of the system is determined by t. Keeping this analogy in mind we will call components of the wave function Ψ simply the partition function Z.

Next, to each step between the two sites we also have to assign a factor depending on the scattering and the magnetic field. This can be easily done for a path with a fixed spin configuration. For example, if $\sigma_n = +1$ and $\sigma_{n+1} = +1$ we have scattering from upper to upper channel and the corresponding factor is $\alpha e^{i\varphi_{n+1}}$. The combination $\sigma_n = +1$, $\sigma_{n+1} = -1$ corresponds to scattering from upper to lower channel which is described by $-\beta^* e^{-i\varphi_{n+1}}$. Similarly, for $\sigma_n = -1$, $\sigma_{n+1} = +1$ we have a factor $\beta e^{i\varphi_{n+1}}$ and for $\sigma_n = -1$, $\sigma_{n+1} = -1$ a factor $\alpha^* e^{-i\varphi_{n+1}}$.

The wave amplitude (partition function) to reach the site (x,t) with an initial condition given by the value of σ_0 is

$$\begin{aligned} Z(x,t) &= \sum_{\sigma_1 \ldots \sigma_t}{}' \prod_{n=0}^{t-1} [\alpha_n e^{i\varphi_{n+1}}]^{\frac{1}{4}(1+\sigma_n)(1+\sigma_{n+1})} [\beta_n e^{i\varphi_{n+1}}]^{\frac{1}{4}(1-\sigma_n)(1+\sigma_{n+1})} \\ &\quad \times [-\beta_n^* e^{-i\varphi_{n+1}}]^{\frac{1}{4}(1+\sigma_n)(1-\sigma_{n+1})} [\alpha_n^* e^{-i\varphi_{n+1}}]^{\frac{1}{4}(1-\sigma_n)(1-\sigma_{n+1})} \\ &= \sum_{\sigma_1 \ldots \sigma_t}{}' e^{i \sum_{n=1}^{t} \varphi_n \sigma_n} \prod_{n=0}^{t-1} \exp\left[\sigma_n \sigma_{n+1} \left(\frac{1}{2} \ln \frac{|\alpha|}{|\beta|} - i \frac{\pi}{4} \right) + \frac{1}{2} \ln |\alpha\beta| + i \frac{\pi}{4} \right. \\ &\quad \left. + i \sigma_n \left(\frac{\arg(\alpha) - \arg(\beta)}{2} + \frac{\pi}{4} \right) + i \sigma_{n+1} \left(\frac{\arg(\alpha) + \arg(\beta)}{2} - \frac{\pi}{4} \right) \right] , \end{aligned} \tag{4.5}$$

where the prime on the summation sign indicates that the partition function Z has to be evaluated for constant magnetization, i.e., under the constraint $\sum_{n=1}^{t} \sigma_n = x$.

In terms of α and β expression (4.5) is still very general and can be used to study layered disorder, i.e., the problem when all scatterers along the same t are equivalent to each other but might be totally independent of scatterers at different t. For dissipationless wave propagation the normalization condition requires $|\alpha|^2 + |\beta|^2 = 1$. If the magnitudes of the α and β are equal, then a wave is scattered into an upper or lower channel with equal probability. Randomness in the ratio $|\alpha|/|\beta|$ will lead to a "random bond" in the one-dimensional Ising model (this will be clarified below). On the other hand, randomness in the arguments of α and β could be interpreted as a random field Ising model. Our goal here is to study new features which come from the magnetic field alone. Thus, we can choose a simple form for matrix elements α and β, for example

$$\alpha = \frac{1}{\sqrt{2}} \qquad \beta = \frac{i}{\sqrt{2}} . \tag{4.6}$$

The choice (4.6) yields

$$Z(x,t) = \left(\frac{1}{\sqrt{2}} \right)^t \sum_{\sigma_1 \ldots \sigma_t}{}' e^{[\, J \sum_{n=0}^{t-1} (\sigma_n \sigma_{n+1} - 1) + i \sum_{n=1}^{t} \varphi_n \sigma_n \,]} , \tag{4.7}$$

where J is defined by relation $e^{-2J} = i$ or $J = -i\frac{\pi}{4}$.

The constrained sums make further progress very difficult. To get rid of this constraint it is convenient to introduce the momentum representation by

$$Z(k,t) = \frac{1}{N}\sum_x Z(x,t)\, e^{-ikx} = \frac{1}{N}\left(\frac{1}{\sqrt{2}}\right)^t \sum_{\sigma_1 \ldots \sigma_t} e^{[\, J\sum_{n=0}^{t-1}(\sigma_n\sigma_{n+1}-1) + i\sum_{n=1}^{t} h_n\sigma_n\,]}, \tag{4.8}$$

where k is one of the $k_m = \frac{2\pi}{N}m$ and $h_n = \varphi_n - k$. It is clear from Eq. (4.8) that a Fourier transform of the amplitude to reach point (x,t) is precisely the partition function for a generalized one-dimensional Ising model. Compared to the ordinary Ising model we have now a complex coupling constant J and the local magnetic field h_n has an imaginary prefactor. The standard Ising model in an inhomogeneous magnetic field was studied in Ref. 16. In our case the complex exponent will lead to some divergences. We shall identify these divergences and present a way to handle them.

The partition function in k space can be written in the form

$$Z(k,t) = Z_+(k,t) + Z_-(k,t) \tag{4.9}$$

where

$$Z_\pm(k,t) = \left(\frac{1}{\sqrt{2}}\right)^t \sum_{\sigma_1 \ldots \sigma_{t-1}} e^{[\, J\sum_{n=0}^{t-2}(\sigma_n\sigma_{n+1}-1) + i\sum_{n=1}^{t-1} h_n\sigma_n + J(\pm\sigma_{t-1}-1) \pm ih_t\,]}\,. \tag{4.10}$$

Z_+ and Z_- are the k-space amplitudes to reach point (x,t) from the upper or lower direction, respectively. It is easy to see that the following recursive relations hold:

$$Z_\pm(n) = \frac{1}{\sqrt{2}} e^{\pm ih_n}\,[\, Z_\pm(n-1) + e^{-2J}\, Z_\mp(n-1)\,]\,. \tag{4.11}$$

Defining the two ratios $r_+(n)$ and $r_-(n)$ by

$$r_\pm(n) = \frac{Z_\mp(n)}{Z_\pm(n)} = e^{\mp 2ih_n}\,\frac{r_\pm(n-1) + e^{-2J}}{e^{-2J}r_\pm(n-1) + 1}, \tag{4.12}$$

after some lengthy but straightforward algebra we find

$$Z_\pm(k,t) = \frac{1}{N}\left(\frac{1}{\sqrt{2}}\right)^t e^{J(\pm\sigma_0 - 1)}\, e^{\mp ikt} \times e^{\pm i\sum_{n=1}^{t}\varphi_n} \prod_{n=1}^{t-1}{}' [\,1 + i\, r_\pm(n)\,]\,. \tag{4.13}$$

The prime on the product sign means that care must be taken when the ratios $r_\pm$ diverge. In what follows we describe how to treat this problem. We start with

$$r_\pm(n=1) = e^{\mp 2J\sigma_0} e^{\mp 2i(\varphi_1 - k)} \tag{4.14}$$

and use Eq. (4.12) to evaluate ratios for larger values of n. If for some n, $r_\pm(n) = e^{-2J} = i$ (yielding a divergent term) then the $(n+1)$th term in the product is set to one and the next two terms in the product are given by

$$r_\pm(n+2) = e^{2J}\,[\,(e^{-4J} - 1)e^{\mp 2i(\varphi_{n+2} - k)} - 1\,] \tag{4.15}$$

and

$$r_\pm(n+3) = e^{2J}\, e^{\mp 2i(\varphi_{n+3} - k)}\,. \tag{4.16}$$

The contributions of terms given by Eqs. (4.15) and (4.16) to the product in Eq. (4.13) are

$$1 + i\, r_\pm(n+2) = -2\, e^{\mp 2i(\varphi_{n+2} - k)} \tag{4.17}$$

and

$$1 + i\, r_\pm(n+3) = 2\cos(\varphi_{n+3} - k) e^{\mp i(\varphi_{n+3} - k)}\,. \tag{4.18}$$

The iterative procedure described above gives a Fourier transform of Z. Returning to the real space by an inverse transform

$$Z_\pm(x,t) = \sum_k Z_\pm(k,t)\, e^{ikx}\,, \tag{4.19}$$

and computing the probability that a wave will end at point (x,t) we find

$$|\, Z(x,t)\,|^2 = |\, Z_+(x,t)\,|^2 + |\, Z_-(x,t)\,|^2\,. \tag{4.20}$$

B. Numerical results and discussion

The expression (4.13) together with Eqs. (4.14)–(4.16) uniquely determine the probability distribution after t steps for any magnetic flux. As is pointed out in Ref. 11, its behavior strongly depends on the commensurability of $\alpha = 2\pi\Phi/\Phi_0$. If $\alpha = p/q$ (p,q are integers), the calculation of the partition function (4.8) can be related to the case when magnetic flux is not present. To show it, we write Eq. (4.8) in the form

$$Z(k,t) = \frac{1}{N}\left(\frac{1}{\sqrt{2}}\right)^t \times \sum_{\sigma_1 \ldots \sigma_t} T(\sigma_0,\sigma_1)T(\sigma_1,\sigma_2)\cdots T(\sigma_{t-1},\sigma_t) \times e^{\frac{i}{2}(\sigma_t h_t - \sigma_0 h_0)}, \tag{4.21}$$

where $T(\sigma_n,\sigma_{n+1})$ is a 2×2 transfer matrix

$$T(\sigma_n,\sigma_{n+1}) = e^{J(\sigma_n\sigma_{n+1}-1) + \frac{i}{2}(\sigma_n h_n + \sigma_{n+1}h_{n+1})}. \tag{4.22}$$

The extra field h_0 is defined because of symmetry and it is set to be zero. The transfer matrices in Eq. (4.21) do not

commute. This is a consequence of their dependence on the magnetic flux (index n is related to our gauge choice). However, for rational α the n dependence can be eliminated. Grouping transfer matrices in Eq. (4.21) into groups with q factors we will get a new set of n/q commuting matrices $T' = T(\sigma_n, \sigma_{n+1}) \cdots T(\sigma_{n+q}, \sigma_{n+q+1})$, which is n independent. The grouping procedure corresponds to the rescaling of our initial lattice with coordinates (x,t) to the new lattice (x',t') so that $x = qx'$ and $t = qt'$. On a rescaled lattice the effect of an external field is apparently eliminated and the problem can be solved as in Sec. III.

Diagonalizing matrix T' yields two eigenvalues $\lambda_{1,2}$ and corresponding eigenvectors $E_{1,2}$ which are orthogonal and normalized

$$E_i^*(+)E_j(+) + E_i^*(-)E_j(-) = \delta_{i,j}, \tag{4.23}$$

where $+/-$ denotes the upper or lower component of the eigenvector E_i. In terms of the eigenvalues and the eigenvectors, the partition function is

$$Z(k,t) = \frac{1}{N}\left(\frac{1}{2}\right)^{\frac{t}{2}} \sum_{\sigma_t} \{\, \lambda_1^{\frac{t}{q}} E_1^*(\sigma_0)E_1(\sigma_t) + \lambda_2^{\frac{t}{q}} E_2^*(\sigma_0)E_2(\sigma_t) \,\}\, e^{\frac{i}{2}(\sigma_t h_t - \sigma_0 h_0)}. \tag{4.24}$$

Equation (4.24) has the same structure as Eqs. (3.11) and (3.12) but, as we have argued, it also describes the effect of rational magnetic flux. In Fig. 2(a) the full line shows the probability distribution for the case when the applied magnetic flux is $\alpha = 1/3$. For this case the matrix T' is built from three T matrices in sequence. The eigenvalues in Eq. (4.23) are

$$\lambda_{1,2} = -2\sin(k)\left[\cos\left(\frac{\pi}{3}\right) + 2\cos^2(k)\right] \pm 2i\sqrt{2 - \sin^2(k)\left[\cos\left(\frac{\pi}{3}\right) + 2\cos^2(k)\right]^2} \tag{4.25}$$

and corresponding eigenvectors

$$E_{1,2} \sim \begin{pmatrix} -e^{-ik}[\sin(2k) - i\,\cos(\frac{\pi}{3})] - \sqrt{2}e^{\pm i\varphi} \\ -\cos(2k) + i\,\sin(\frac{\pi}{3}) \end{pmatrix}, \tag{4.26}$$

where $\varphi = \arg(\lambda_+)$.

From Figs. 2(a) and 2(b) we see that increasing "magnetic flux" causes the beam to become more collimated. The general form of the probability distribution remains unchanged. This is precisely what one would expect following the above arguments. Namely, by introducing magnetic flux we effectively rescale our lattice to some smaller lattice (x',t'). Smaller t leads to smaller diffusion. Diffusion of the propagating wave as a function of t is discussed in Sec. III.

The behavior of the probability distribution is very sensitive to the value of α. Even small changes from rational α to some close irrational number produce dramatic effects. In Figs. 2(a) and 2(b), the probability distributions after $t = 100$ steps are compared for $\alpha = 1/3 = 0.333\ldots$, $\frac{1}{\sqrt{8}} = 0.353\ldots$ and $\alpha = 0.6$, $\frac{\sqrt{5}-1}{2} = 0.618\ldots$. For

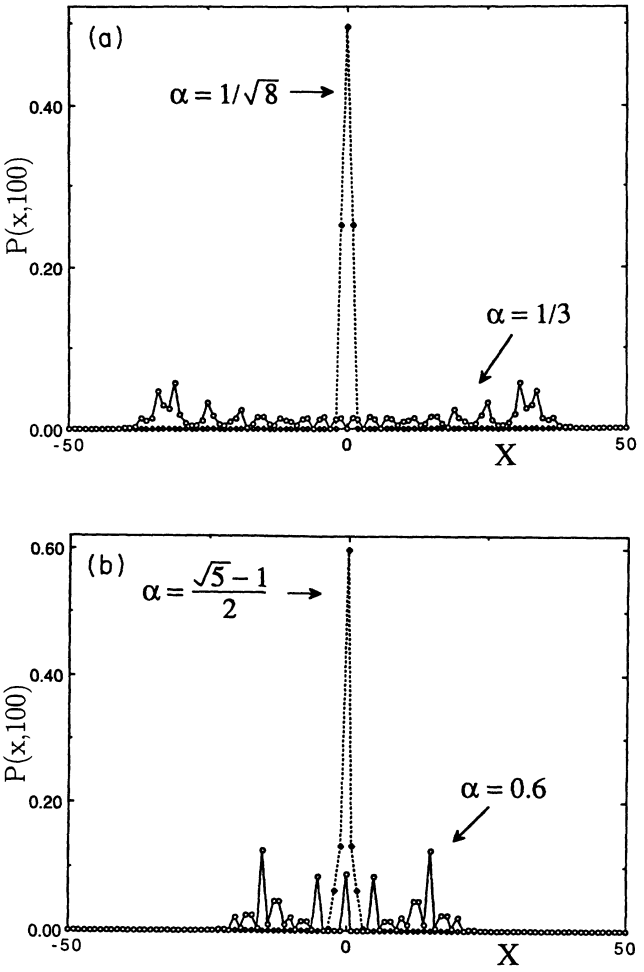

FIG. 2. The behavior of $P(x,t)$ for $t = 100$ and $-50 \le x \le 50$ for rational and irrational values of α: **(a)** $\alpha = 1/3$ (full line) and $\alpha = 1/8^{1/2}$ (broken line); **(b)** $\alpha = 0.6$ (full line) and $\alpha = (5^{1/2} - 1)/2$ (the golden mean) (broken line).

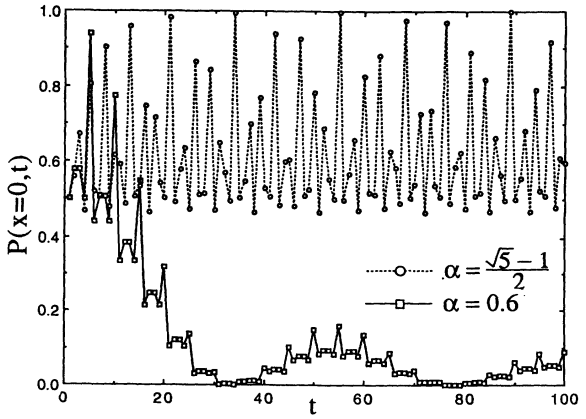

FIG. 3. The behavior of $P(x,t)$ for $x = 0$ and $0 \le t \le 100$ for $\alpha = 0.6$ and $(\sqrt{5} - 1)/2$.

irrational α, the distribution is concentrated at the small region around $x = 0$. The probability of reaching point $x = 0$ as a function of t is shown in Fig. 3 for rational and irrational α. While for rational α $P(x = 0, t)$ decays with regular oscillations, irrational α produces an aperiodic structure which does not decay with t. The high sensitivity to irrational α could be traced back to Eq. (4.18) giving the product of $\cos(\pi\alpha n)$ factors. Recently, in Ref. 12, the behavior of the localized electrons on a lattice with incommensurate magnetic flux was investigated. The general features we find here are similar to those derived in Ref. 12.

V. DIRECTED WAVES IN STRONGLY DISORDERED MEDIA

In this section, we discuss the wave propagation in a random medium. We describe the randomness by taking the scattering matrix at each lattice site to be an independent random element of the $U(2)$ group. We are interested in the behavior of the probability distribution and its higher moments as well as the transverse moments of x, i.e., $[\langle x^n\rangle]$ and $[\langle x\rangle^n]$ as functions of the longitudinal distance t. To calculate $[\langle x\rangle^n]$ one needs to know the correlations among n paths propagating on the lattice with a given realization of randomness. These correlations are the primary subject of our interest. Using some simple formulas for group integration we will develop a systematic and exact procedure for averaging various quantities of physical interest over the disorder.

The probability $P(x,t)$ of reaching a given point (x,t) can be calculated by summing over all possible paths which begin at the origin and end at (x,t). Denoting by $A_i(x,t)$ the contribution of the ith path, the probability $P(x,t)$ is given by

$$P(x,t) = \left|\sum_i A_i(x,t)\right|^2 = \sum_{i_1,i_2} A^*_{i_1}(x,t)\, A_{i_2}(x,t)\ . \quad (5.1)$$

The amplitude A_i is simply the product of t random, mutually independent elements of the S matrices along the ith path. All amplitudes are defined for the same realization of the disorder. The contributions of two paths i_1 and i_2 to the sum in (5.1) depend on their mutual relation. The two paths can be totally disconnected (meeting only at the end points), they can overlap along some links, or intersect at some lattice sites. On their common parts they share the same factors. From a statistical point of view, the most interesting phenomena are related to intersections and merging or branching points. At these points, paths do not have assigned the same factors but factors from the same scattering matrices.

We now turn to the question of the statistical averaging over the quenched disorder. We assume a uniform distribution of S matrices over all unitary matrices. Hence, with an equal probability the scattering matrix may be any $U(2)$ matrix. In this case there is no difference between averaging over either the $U(2)$ or the $SU(2)$ group. Other choices, such as distributions preferring some propagating direction, are also possible, but will not be discussed here.

The quenched average of the probability distribution P over all realization of the disorder is straightforward to compute. After averaging, only the paired or neutral paths (such that one member is selected from A^*_i and the other from A_i) give a nonzero contribution to the sum in Eq. (5.1). Using the following integral over the $SU(N)$ group[18]

$$\int dS\, S_{ij} S^*_{lk} = \frac{1}{N}\delta_{jk}\delta_{il}, \quad (5.2)$$

with $N = 2$ and counting the number of different paths from the origin to the point (x,t) we obtain

$$[P(x,t)] = \frac{1}{2^t}\frac{t!}{(\frac{t+x}{2})!(\frac{t-x}{2})!}\ . \quad (5.3)$$

This formula is all that is needed to calculate all transverse moments $[\langle x^n\rangle]$. We are particularly interested in the second moment characterizing the beam position. In this case, Eq. (5.3) gives

$$[\langle x^2(t)\rangle] = \sum_x x^2[P(x,t)] = t\ . \quad (5.4)$$

The result (5.4) was already derived in Refs. 7 and 8 and is also in agreement with our numerical simulations shown in Fig. 4. It describes the ordinary diffusion of a classical particle in a stochastic medium. Classical diffusion is naturally expected since in Eq. (5.3) there is no contribution from intersecting paths. Comparing with the pure case (3.13), we conclude that averaging over randomness removes the interference effects in P. The probability distribution P for propagation over nonrandom and random scatterers is shown in Fig. 5. For the random case averaging was performed on 500 samples. By increasing the number of samples the curve becomes smoother showing no effect of interference.

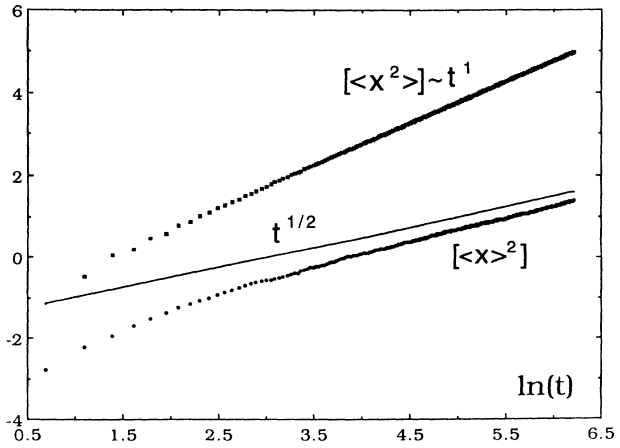

FIG. 4. Log-log plots of $[\langle x^2\rangle]$ and $[\langle x\rangle^2]$ for $t \le 500$. The former fits a linear t behavior within 10^{-3} accuracy. The expected $t^{\frac{1}{2}}$ asymptotic behavior of the latter is also depicted (full line).

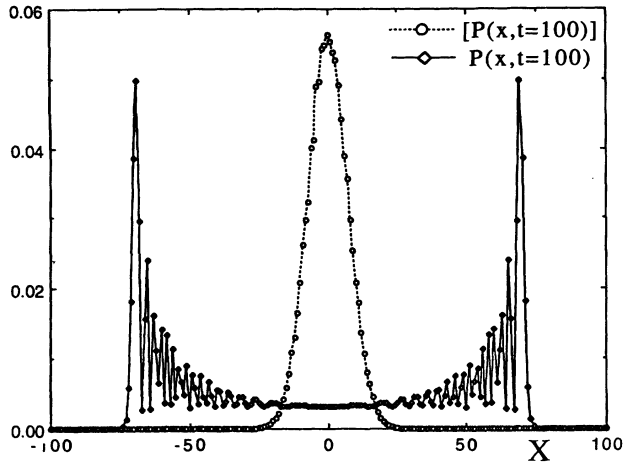

FIG. 5. Comparison of $P(x,t)$ for $t = 100$ and $-50 \leq x \leq 50$ for the pure case (full line) and the random case (broken line). The disorder average is done over 500 realizations.

Nontrivial problems arise if one tries to find the scaling properties of the beam center $[\langle x\rangle^2]$. Results of long time Monte Carlo simulations are shown in Fig. 4. Our numerical results are consistent with those given in Ref. 6 but the value of the scaling exponent is still unclear. Computer simulations with larger t and more samples could help to resolve this uncertainty. However, Saul, Kardar, and Read[7] suggested a way to reduce numerical difficulties. They proposed to construct recursion relations among exactly averaged quantities at different t. We will follow their approach.

The basic idea is to calculate the correlation functions averaged over the disorder. They are defined by

$$W_n(x_1,\ldots,x_n,t) = [P(x_1,t)\ldots P(x_n,t)] \,. \tag{5.5}$$

For $n = 1$, $W_1(x,t)$ is given by (5.1). It describes the time evolution of one neutral path made up of a segment going from origin to (x,t) and its complex conjugate which can be viewed as the time evolution in the opposite direction. For $n \geq 2$ Eq. (5.5) gives the probability that n neutral paths starting at the origin will end at position $(x_1,x_2,\ldots,x_n)$ at distance t. Some characteristic configurations for time evolution of W_2, W_3, and W_4 are shown in Fig. 6. W_n must satisfy the initial conditions

$$W_n(x_1,x_2,\ldots,x_n,t=0) = \delta_{x_1,0}\delta_{x_2,0}\ldots\delta_{x_n,0} \,, \tag{5.6}$$

as well as a sum rule which is a consequence of the probability conservation

$$\sum_{x_1}\sum_{x_2}\cdots\sum_{x_n} W_n(x_1,x_2,\ldots,x_n,t) = 1 \,. \tag{5.7}$$

The role of W_n in calculation of $[\langle x\rangle^n]$ is seen from the following relation:

$$[\langle x\rangle^n] = \sum_{x_1}\sum_{x_2}\cdots\sum_{x_n} x_1x_2\cdots x_n \times[P(x_1,t)P(x_2,t)\cdots P(x_n,t)] \,. \tag{5.8}$$

Evaluation of W_n is based on the recursion relations connecting W_n at distance t and $t+1$. The recursion relations can be derived by using symmetry arguments and recalling that only neutral paths can survive disorder averaging. The neutral paths, however, may cross each other and exchange partners as in Fig. 6. The exchange effect means that we are dealing with interacting paths. It is convenient at this point to introduce relative coordinates $(x,r_1,r_2,\ldots r_{n-1})$ instead of the previous set $(x_1,x_2,\ldots x_n)$. The coordinate r is the distance between paths at some specified t (see Fig. 6). The calculation of $W_2(x,r)$ is relatively simple. First, we look for all different ways to construct $W_2(x,r,t+1)$ from $W_2(x,r,t)$. Neglecting the crossings at t there are four possibilities as is shown in Fig. 7. $W_2(x,r,t+1)$ is, therefore, a combination of $W_2(x\pm1,r,t)$ and $W_2(x\pm1,r\pm1,t)$. The next step is to include the effects of path exchange. They are present only if $r = 0,\pm1$ at t. This leads to the following terms in the recursion relation:

$$\frac{1}{4}(1+\epsilon_0\delta_{r,0})W_2(x\pm1,r,t), \tag{5.9}$$

$$\frac{1}{4}(1+\epsilon_1\delta_{r,\mp1})W_2(x\pm1,r\pm1,t), \tag{5.10}$$

where we have parametrized the effect of disorder by ϵ_0 and ϵ_1. Due to the symmetry $r \to -r$, the coefficients of $W_2(x+1,r+1,t)$ and $W_2(x-1,r-1,t)$ must be equal. This observation, although trivial for W_2, is very useful for calculation of W_n for higher n. The sum rule (5.7) implies that the sum of all the coefficients must be equal to one yielding $\epsilon_0 = -\epsilon_1$. Thus, the recursion relation for W_2 can be written in the form:

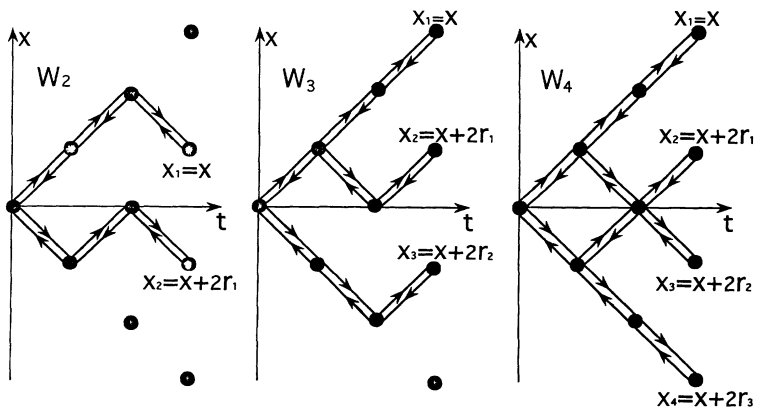

FIG. 6. Some typical configurations contributing to W_2, W_3, and W_4. Arrow directions indicate paths which belong to A_i or to A_i^*. Also shown are the relations between the coordinate set $(x_1,\ldots,x_n)$ and the set $(x,r_1,\ldots,r_{n-1})$.

$$W_2(x,r,t+1) = \tfrac{1}{4}(1+\epsilon\delta_{r,0})\{\, W_2(x+1,r,t) + W_2(x-1,r,t)\}$$
$$+\tfrac{1}{4}(1-\epsilon\delta_{r,1})W_2(x-1,r-1,t) + \tfrac{1}{4}(1-\epsilon\delta_{r,-1})W_2(x+1,r+1,t)\,. \quad (5.11)$$

The left-hand side of Eq. (5.11) may be directly calculated by averaging the quantity $[P(x_1,t+1)P(x_2,t+1)]$ over the $SU(2)$ group. This is easily done for small t since the number of possible configurations which must be taken into account is relatively small. In addition to the result (5.2), we also need a formula for an integral over four $SU(2)$ elements[18]

$$\int dS\, S_{ij}S^*_{lk}S_{mn}S^*_{qp} = \frac{1}{N^2-1}(\delta_{il}\delta_{mq}\delta_{jk}\delta_{np} + \delta_{iq}\delta_{ml}\delta_{jp}\delta_{nk}) + \frac{1}{N(N^2-1)}(\delta_{il}\delta_{mq}\delta_{jp}\delta_{nk} + \delta_{iq}\delta_{ml}\delta_{jk}\delta_{np})\,. \quad (5.12)$$

It turns out that $\epsilon = \frac{1}{3}$. The same procedure can be used for a systematic evaluation of other correlation functions. In the Appendix we give the results for W_3 and W_4.

Now we investigate the t scaling of $W_n(x = r_1 = \cdots = x_{n-1} = 0,t)$ and $\sum_x W_n(x, r_1 = r_2 = \cdots = r_{n-1} = 0,t)$. In the language of random walk the former quantity is the probability that n paired paths will reach the same point $x = 0$ after time t and the latter is the probability of their reunion somewhere [see Eq. (5.5)]. The defining equation of W_n, (5.5), gives

$$\sum_x W(x, r_1 = r_2 = \cdots = r_{n-1} = 0, t) = \sum_x [P(x,t)^{n-1}P(x,t)] \quad (5.13)$$

which are exactly the moments of the probability distribution itself. Recently it was argued by Bouchaud *et al.*[10] that the evolution of the wave must be described by an infinite set of exponents defined by

$$\sum_x [P(x,t)] \approx t^{\mu(n)}\,. \quad (5.14)$$

The nontrivial form of the function $\mu(n)$ is a sign of the "multifractal" structure of the propagating wave. For $n = 2,3,4$ the behavior of the μ can be found simply by iterating the recursion relations (5.5), (A1), and (A2)

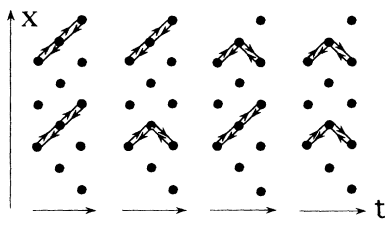

FIG. 7. All possible step configurations of noninteracting pairs of paths advancing from $t-1$ to $t+1$.

numerically. The numerical results shown in Fig. 8 and Fig. 9 suggest that for large t

$$W_n(x = r_1 = \cdots = r_{n-1} = 0, t) \sim t^{-\frac{n}{2}} \quad (5.15)$$

$$\sum_x W_n(x, r_1 = \cdots = r_{n-1} = 0, t) \sim t^{-\frac{n}{2}+\frac{1}{2}}\,. \quad (5.16)$$

These relations indicate that for large t the interaction among paths is irrelevant.[19]

The recursion relation (5.11) for $W_2(r=0,t)$ can be diagonalized for small ϵ. The nonperturbed eigenvectors are sin or cos functions and matrix elements of ϵ-dependent terms in Eq. (5.11) are

$$V_{nm} = \delta_{n,0}\{\, \tfrac{1}{2}\epsilon\delta_{m,o} - \tfrac{1}{4}\epsilon\delta_{|m|,1}\,\}. \quad (5.17)$$

The eigenvalues of the transfer matrix relating $W_2(r = 0,t+1)$ and $W_2(r=0,t)$ are

$$\lambda_\pm(k_m) = \cos^2\left(\frac{k_m}{2}\right)\left\{1 \pm \epsilon\,\frac{4}{2N+1}\sin^2\left(\frac{k_m}{2}\right)\right\} + O(\epsilon^2), \quad (5.18)$$

where $k_m = \frac{2\pi}{2N+1}m$, $m = 0, \pm1, \ldots \pm N$. For large t, the eigenvalues (5.18) and corresponding eigenvectors yield

$$W_2(r=0,t) = \frac{1}{2^{2t}}\binom{2t}{t} + O\left(\frac{\epsilon}{\sqrt{t}}\right). \quad (5.19)$$

Equation (5.19) shows that the effect of ϵ is too local to produce any relevant effect for large N. This supports the predicted scaling behavior in Eqs. (5.15) and (5.16).

VI. CONCLUSIONS

In this work we studied different aspects of a lattice model for unitary propagation. We first presented a closed-form solution for such a propagation in a uniform

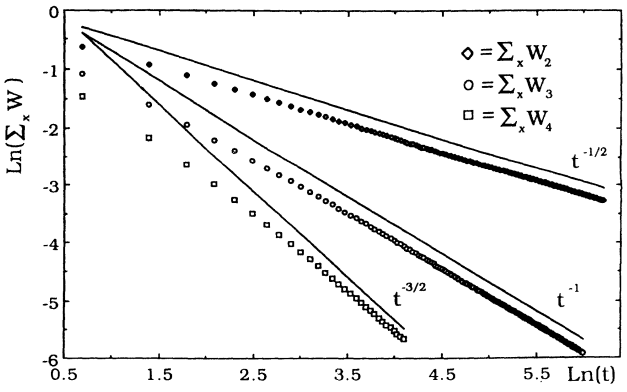

FIG. 8. Log-log plot for moments of the probability distribution versus t, compared with their conjunctured large t behaviors (full lines).

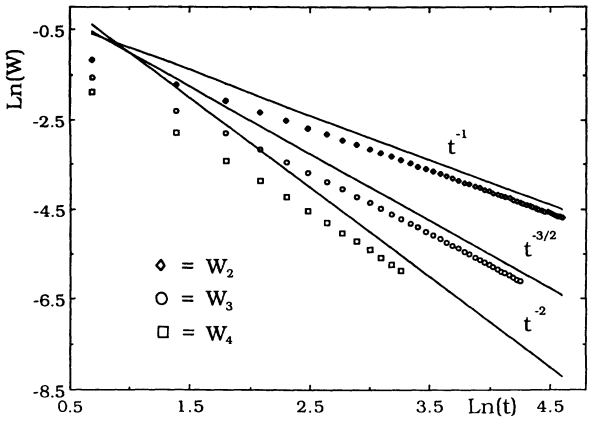

FIG. 9. Log-log plot for the probability that n paths will end at the same point $x = 0$ after a distance t. The full lines indicate the conjunctured large t behaviors.

medium. Then we took a theoretical "detour" to study the case when the phases were modulated as if they were due to an external magnetic field. As emphasized before, this situation does not describe lattice electrons with a field in 1D or 2D. It is rather an interesting theoretical extension of the "directed paths" model of localized lattice electrons in 2D, which can widen our general understanding of this important class of systems. For the nonunitary model, the complete solution was found.[11,15] Interesting inflation rules were found for $\Phi/\Phi_0 = p/q$. For incommensurate Φ/Φ_0 an aperiodic behavior with striking scaling properties was revealed.[12] In the unitary case studied here, we have shown that the model cannot be solved completely by straightforward application of transfer matrix techniques but we managed to find a closed form for the probability distribution of propagating waves by mapping our problem to a generalized Ising model with an imaginary coupling constant J and an imaginary inhomogeneous external field. The problem was also investigated numerically. Inflation rules for rational p/q hold in this case too but they are certainly not as trivial. The wave function amplitude becomes more and more "collimated" around $x = 0$ as q is increased.

We next studied the disordered case. Because of the "light cone" constraint on the lattice we have found $\langle x^2 \rangle \sim t$, while the behavior off lattice is known to be $\langle x^2 \rangle \sim t^3$.[9] So in the presence of disorder the present lattice model does not recover the continuum limit. The continuum analysis was performed on the Schrödinger equation for a particle moving in a random potential which changes rapidly both in space and in time. Our results for $[\langle x \rangle^2]$ agree with that of Saul *et al.*[7]

We have also investigated the higher moments of $P(x,t)$. Our numerical investigations were based on the recursion relations between various moments. It should be emphasized that the averaging over disorder leads to exact (but cumbersome) relations that are then iterated numerically (the iteration process does not involve randomness anymore). Our numerical results suggest a simple "gap scaling" $[P^n(x,t)] \sim t^{-\frac{n}{2}}$. A simple analytic argument explains this behavior for $n = 2$, (see also Ref. 7). Although we cannot prove it rigorously, it looks very likely that these analytic arguments hold for $n > 2$ as well. How can we reconcile this gap scaling with the multifractal behavior found by Bouchaud *et al.*? In their model the wave function is defined on the sites and unitarity was ensured by replacing the evolution operator $e^{-\frac{i}{\hbar}\hat{\mathcal{H}}t}$ by the Cayley operator $(1 - \frac{i}{\hbar}\hat{\mathcal{H}}t)/(1 + \frac{i}{\hbar}\hat{\mathcal{H}}t)$. So the most likely possibility that comes to mind is that the behavior is very sensitive to the type of latticization used. The fact that neither lattice formulation yields the correct continuum limit leaves open the unusual situation in which different lattice models may belong to different universality classes. It should be also pointed out that the deviations from gap scaling found in Ref. 10 are very small for these positive moments but are substantial for negative moments which are not studied here. More investigations of this and related issues will be most worthy.

ACKNOWLEDGMENT

We are grateful to M. Kardar for useful conversations and critical reading of the manuscript. We are also thankful to J.P. Bouchaud and E. Medina for clarifying comments. Acknowledgment is made to the donors of the Petroleum Research Fund, administrated by the ACS, for support of this research.

APPENDIX: RECURSION RELATIONS FOR W_3 AND W_4

Here we present the recursion relations for the correlation functions $W_3(x, r_1, r_2, t)$ and $W_4(x, r_1, r_2, r_3, t)$. The derivation is completely analogous to the one described in Sec. V for $W_2(x, r, t)$. However, for given coordinates of the ending point at distance t there are now many more path configurations contributing to W which make the calculation somewhat tedious. For W_3 one finds

$$W_3(x, r_1, r_2, t+1) = \frac{1}{8}\sum_a W_3(x + a_0, r_1 + a_1, r_2 + a_2, t) \times \{1 + \tfrac{1}{3}[(-1)^{a_1}\delta_{r_1+a_1,0} + (-1)^{a_2}\delta_{r_2+a_2,0} + (-1)^{a_1+a_2}\delta_{r_1+a_1,r_2+a_2}]\} \quad \text{(A1)}$$

where the sum is over $a = (a_0, a_1, a_2) = (\pm 1, 0, 0), (\pm 1, \pm 1, 0), (\pm 1, 0, \pm 1), (\pm 1, \pm 1, \pm 1)$. Similarly the recursion relation for W_4 reads

$$W_4(x,r_1,r_2,r_3,t+1) = \frac{1}{16}\sum_a W_4(x+a_0,r_1+a_1,r_2+a_2,r_3+a_3,t)\ \{1+\tfrac{1}{3}[(-1)^{a_1}\delta_{r_1+a_1,0}$$
$$+(-1)^{a_2}\delta_{r_2+a_2,0}+(-1)^{a_3}\delta_{r_3+a_3,0}+(-1)^{a_1+a_2}\delta_{r_1+a_1,r_2+a_2}$$
$$+(-1)^{a_1+a_3}\delta_{r_1+a_1,r_3+a_3}+(-1)^{a_2+a_3}\delta_{r_2+a_2,r_3+a_3}]$$
$$+\tfrac{1}{9}(-1)^{a_1+a_2+a_3}[\delta_{r_1+a_1,0}\delta_{r_2+a_2,r_3+a_3}+\delta_{r_2+a_2,0}\delta_{r_1+a_1,r_3+a_3}$$
$$+\delta_{r_3+a_3,0}\delta_{r_1+a_1,r_2+a_2}]-\tfrac{2}{15}(-1)^{a_1+a_2+a_3}\delta_{r_1+a_1,0}\delta_{r_2+a_2,0}\delta_{r_3+a_3,0}\ \}, \qquad \text{(A2)}$$

where $a = (a_0,a_1,a_2,a_3) = (\pm1,0,0,0),(\pm1,\pm1,0,0),(\pm1,0,\pm1,0),(\pm1,0,0,\pm1),(\pm1,\pm1,\pm1,0),(\pm1,\pm1,0,\pm1),(\pm1,0,\pm1,\pm1),(\pm1,\pm1,\pm1,\pm1)$.

---

[1] S. M. Rytov and Yu. A. Kravtsov, *Principles of Statistical Radiophysics* (Springer-Verlag, New York, 1987).
[2] Yu. A. Kravtsov, *Geometrical Optics of Inhomogeneous Media* (Springer-Verlag, New York, 1990).
[3] A. Ishimaru, *Wave Propagation and Scattering in Random Media* (Academic, New York, 1978).
[4] R. Dashen, J. Math. Phys. **20**, 894 (1979).
[5] S. Feng, L. Golubovic, and Y.-C. Zhang, Phys. Rev. Lett. **65**, 1028 (1990).
[6] E. Medina, M. Kardar, and H. Spohn, Phys. Rev. Lett. **66**, 2176 (1991).
[7] L. Saul, M. Kardar, and N. Read, Phys. Rev. A **45**, 8859 (1992).
[8] A.A. Ovchinnikov and N.S. Erikhman, Zh. Eksp. Teor. Fiz. **67**, 1474 (1974) [Sov. Phys. JETP **40**, 733 (1975)].
[9] A. M. Jayannavar and N. Kumar, Phys. Rev. Lett. **48**, 553 (1982).
[10] J.P. Bouchaud, D. Touati, and D. Sornette, Phys. Rev. Lett. **68**, 1787 (1992).
[11] Y. Shapir and X.R. Wang, Mod. Phys. Lett. B **4**, 1301 (1990).
[12] S. Fishman, Y. Shapir, and X.R. Wang, Phys. Rev. B **46**, 12 154 (1992).
[13] V. L. Nguyen, B. Z. Spivak, and B. I. Shklovskii, Pis'ma Eksp. Teor. Fiz. **41**, 35 (1985) [JETP Lett. **41**, 42 (1985)].
[14] Y. Shapir and X.R. Wang, Europhys. Lett. **4**, 1165 (1987).
[15] E. Medina, M. Kardar, Y. Shapir, and X. R. Wang, Phys. Rev. Lett. **64**, 1816 (1990).
[16] B. Derrida, M.M. France, and J. Peyriere, J. Stat. Phys. **45**, 438 (1986).
[17] H. Gerch, Int. J. Theor. Phys. **20**, 491 (1981); A.L. Kholodenko, J. Stat. Phys. **65**, 291 (1991).
[18] M. Creutz, J. Math. Phys. **19**, 2043 (1978); **68**, 1787 (1992).
[19] M.E. Fisher, J. Stat. Phys. **34**, 667 (1984).